Protein Science (1998), 7:2522–2532. Cambridge University Press. Printed in the USA.

Identification of kinetically hot residues in proteins

MELIK C. DEMIREL,[1] ALI RANA ATILGAN,[1] ROBERT L. JERNIGAN,[2]
BURAK ERMAN,[3] AND IVET BAHAR[1,2]

[1]Polymer Research Center, Bogazici University, and TUBITAK Advanced Polymeric Materials Research Center, Bebek 80815, Istanbul, Turkey
[2]Molecular Structure Section, Laboratory of Experimental and Computational Biology, Division of Basic Sciences, National Cancer Institute, National Institutes of Health, Bethesda, Maryland 20892-5677
[3]Sabanci University, Sabanci Center 80745, and TUBITAK Advanced Polymeric Materials Research Center, Bebek 80815, Istanbul, Turkey

(RECEIVED February 20, 1998; ACCEPTED June 26, 1998)

Abstract

A number of recent studies called attention to the presence of kinetically important residues underlying the formation and stabilization of folding nuclei in proteins, and to the possible existence of a correlation between conserved residues and those participating in the folding nuclei. Here, we use the Gaussian network model (GNM), which recently proved useful in describing the dynamic characteristics of proteins for identifying the kinetically hot residues in folded structures. These are the residues involved in the highest frequency fluctuations near the native state coordinates. Their high frequency is a manifestation of the steepness of the energy landscape near their native state positions. The theory is applied to a series of proteins whose kinetically important residues have been extensively explored: chymotrypsin inhibitor 2, cytochrome *c*, and related C2 proteins. Most of the residues previously pointed out to underlie the folding process of these proteins, and to be critically important for the stabilization of the tertiary fold, are correctly identified, indicating a correlation between the kinetic hot spots and the early forming structural elements in proteins. Additionally, a strong correlation between kinetically hot residues and loci of conserved residues is observed. Finally, residues that may be important for the stability of the tertiary structure of CheY are proposed.

Keywords: CheY; chymotrypsin inhibitor; conserved residues; cytochrome *c*; folding pathway; hot residues; thermal fluctuations; vibrational dynamics

A number of single domain, small proteins are known to fold and unfold according to a two-state kinetics (Schmid, 1992; Fersht et al., 1994; Karplus et al., 1995; Fersht, 1997; Zwanzig, 1997), while kinetic intermediates, or molten globule states generally form under mild denaturing conditions (Kim & Baldwin, 1990; Ptitsyn, 1995). A typical example observed, both experimentally (Jackson et al., 1993; Otzen et al., 1994; Itzhaki et al., 1995) and from molecular dynamics simulations (Li & Daggett, 1996; Daggett et al., 1996), to obey a two-state kinetics, is the chymotrypsin inhibitor 2 (CI2). The latter folds without accumulation of an intermediate or stepwise formation of secondary and tertiary structure.

The two-state folding of small proteins has been attributed to a nucleation-condensation mechanism (Abkevich et al., 1994; Fersht, 1997). According to this mechanism, there is a weak local nucleus which may be represented by a few residues. The latter is stabilized by nonlocal, tertiary contacts. Also it has been shown that the embryonic secondary structure and stabilizing long-range contacts concurrently form the tertiary structure. This description departs from both the framework model of folding (Ptitsyn & Rashin, 1975; Kim & Baldwin, 1990), which proposes the sequential formation of secondary and tertiary structures, and the hydrophobic collapse model (Dill et al., 1995) in which the secondary structure appears as a consequence of the overall condensation of the structure.

Although the nucleation-condensation mechanism generally pertains to the two-state kinetics of small proteins, it is conceivable that the same type of cooperativity between local propensities and tertiary contacts may be operative in the folding of independent structural units, or domains, in larger proteins. Theoretical and experimental studies further suggest that there may be a correlation between residues that are positionally conserved, and those revealed through protein engineering to play a key role in stabilizing tertiary folds. A method for predicting the kinetically important residues and supporting the existence of such a correlation was proposed by Shakhnovich et al. (1996). Therein, the most conserved residues of CI2 were found to be A35, I39, L68, V70, and I76, in agreement with experiments (Fersht, 1997); A35 participates in a nucleus on an α-helix, stabilized by contacts with L68 and I76.

Reprint requests to: Robert L. Jernigan, Molecular Structure Section, Laboratory of Mathematical Biology, Division of Basic Sciences, National Cancer Institute, National Institutes of Health, MSC 5677, Room B-116, Bldg. 12B, Bethesda, Maryland 20892-5677; e-mail: jernigan@structure.nci.nih.gov.

There is apparently a mechanism by which a nucleus, whose vital contacts are instituted upon passage over a transition state, preserves its structure throughout its path to the native state, possibly through a funnel-like energy landscape. The energy localization at residues forming the nucleus may be a reliable instrument preventing the transfer of energy from these to other residues. In fact, energy transfer to neighbors may be strongly hindered in the presence of nonperiodic, or disordered interactions, as first pointed out by Anderson (1958, 1978). Depending on the three-dimensional configuration, especially for medium-to-high-frequency modes (Dean & Bacon, 1963; Sayar et al., 1997), the mode shapes localize at certain loci, which may be termed "kinetically hot spots."

Recently, we developed an analytical method for determining the dynamic characteristics of protein fluctuations in the folded state (Bahar et al., 1997, 1998a, 1998b; Haliloglu et al., 1997). The method, referred to as the Gaussian network model (GNM), is based on contact distributions in the folded state. The spectrum of vibrational modes ranging from fast fluctuations of isolated, individual residues, to cooperative, global motions of large domains, is obtained by eigenvalue analysis of the so-called Kirchhoff matrix of contacts, characteristic of each tertiary fold, as illustrated in the Appendix for a simple model chain. Our approach bears a close resemblance to an earlier study of Holm and Sander (1994). Therein, the slowest modes of motion were considered for identifying structural domains of proteins. Here, we concentrate on the fastest modes.

The fast modes of motion provide information about the kinetically hot residues. These are tightly packed residues, in general. They are trapped in severely constrained minima on the conformational energy landscape. We note that the term "hot spots" was used by Shoemaker et al. (1997) for describing the highly ordered contacts in the transition state underlying the folding nucleus; and the term "kinetically important positions" was proposed by Shakhnovich et al. (1996) for qualifying the most strongly constrained and, thereby, conserved residues in designed sequences. The kinetically hot residues presently predicted by the GNM will indeed be compared with the residues detected by experiments as folding nuclei and/or to be highly conserved.

In the following section, the model and method will be presented in some detail, together with its application to chymotrypsin inhibitor 2 (CI2), a protein whose dynamic characteristics have been studied both experimentally (Jackson et al., 1993; Fersht et al., 1994; Otzen et al., 1994; Itzhaki et al., 1995; Neira et al., 1997) and theoretically (Daggett et al., 1996; Li & Daggett, 1996; Shakhnovich et al., 1996). A perfect agreement between the kinetically hot residues identified by the GNM, and those previously pointed out to underlie the nucleation-condensation mechanism will be observed.

Calculations will be repeated for a series of cytochrome *c*'s and related C2 proteins, and for the chemotactic protein from *Escherichia coli*, CheY (Table 1). In contrast to CI2, which folds via a two-state mechanism, the folding/unfolding of cytochrome *c* involves intermediate states that have been observed by hydrogen exchange labeling coupled with NMR (Roder et al., 1988; Jeng & Englander, 1991; Bai et al., 1995; Kuroda et al., 1995; Sosnick et al., 1996), small angle X-ray scattering (Kataoka et al., 1993), time-resolved circular-dichroism, and fluorescence (Elöve et al., 1992). Here several proteins from the cytochrome *c* family will be considered, to further investigate the possible relationship between conserved residues and folding nuclei. Overall, a correlation will be pointed out between the kinetically hot residues, on the one hand, and formation and stabilization of folding nuclei, and beyond this, the conservation of residues.

Methods

Theory and illustration for chymotrypsin inhibitor 2

General description of the GNM and assumptions

The GNM is based on the following postulate (Bahar et al., 1997; Haliloglu et al., 1997): In folded proteins, residues undergo Gaussianly distributed fluctuations around their mean positions, due to harmonic potentials between all "contacting" residues. No residue specificity need be invoked as a first order approximation. Instead, the inter-residue potentials are all represented by the same single-parameter (γ) harmonic potential, as first proposed by Tirion (1996). Accordingly, the fluctuations Δr_{ij} in distances between C_i^α and C_j^α are controlled by the potential $V = \frac{1}{2}\gamma(\Delta r_{ij})^2$, α-carbons being used as representative sites for residues. The dynamic characteristics of the molecule are fully described in this model by the so-called Kirchhoff matrix $\mathbf{\Gamma}$ of contacts, the elements of which are

$$\Gamma_{ij} = \begin{cases} H(r_c - r_{ij}) & i \neq j \\ -\sum_{i(\neq j)}^{N} \Gamma_{ij} & i = j \end{cases}. \qquad (1)$$

Here N is the total number of residues, r_{ij} denotes the distance between the i^{th} and j^{th} C^α-atoms, and $H(x)$ is the Heaviside step function given as $H(x) = -1$ for $x > 0$ and $H(x) = 0$ for $x \leq 0$.

Table 1. *Proteins in the present study*

PDB code	Full Name	Resolution (Å)	N	Reference
2ci2	Chymotrypsin inhibitor 2 (fragment 19–83)	2.0	64	McPhalen & James (1987)
1hrc	Horse heart cytochrome	1.9	105	Bushnell et al. (1990)
1ccr	Cytochrome *c* from rice embryo	1.5	111	Ochi et al. (1983)
1cot	C2 isolated from *P. denitrificans*	1.7	129	Benning et al. (1994)
1cxa	C2 complexed with imidazole	2.2	124	Axelrod et al. (1994)
1cry	C2 from *Rhodopseudomonas viridis*	3.0	107	Miki et al. (1994)
5cyt	Cytochrome *c* from albacore tuna heart	1.5	103	Takano (1984)
3c2c	*Rodospirillum rubrum* cytochrome C2	1.68	112	Salemme et al. (1973)
3chy	*E. coli* CHE-Y	1.66	129	Volz & Matsumura (1991)

Defined in this way, r_c is the cut-off distance or upper limit for the separation between two "contacting" residues.

The value $r_c = 7$ Å has been adopted in previous applications of the GNM to proteins. This distance includes neighbors within the first coordination shell around a central residue, as revealed from analyses of known structures (Miyazawa & Jernigan, 1996; Bahar & Jernigan, 1997). Alternatively, one could select a broader distance, particularly in proteins containing β-sheets, so as to include the hydrogen-bond forming residue pairs of adjacent strands. The contact map for CI2 is shown in Figure 1. CI2 consists of a four-stranded β-sheet packed against an α-helix, with a wide loop between strands 2 and 3, which contains the reactive site. The secondary structure elements are shown along the axes of Figure 1. The horizontal and vertical bars in the map indicate the nonzero elements of $\mathbf{\Gamma}$ obtained from the crystal structure (McPhalen & James, 1987) using $r_c = 7$ and 10 Å, respectively. Residue indices are in the range $19 \leq i \leq 83 = N$, corresponding to the numbers assigned in the crystal structure.

The i^{th} diagonal element of $\mathbf{\Gamma}$ provides a measure of the local packing density near residue i, in terms of its coordination number, and the trace of $\mathbf{\Gamma}$ divided by N gives the mean coordination number of the residues. Its inverse, $\mathbf{\Gamma}^{-1}$, yields the correlations between the thermal fluctuations of the C^{α} atoms near the native state (Bahar et al., 1997); the diagonal elements of $\mathbf{\Gamma}^{-1}$ scale with the mean-square (MS) fluctuations $\langle \Delta \mathbf{R}_i^2 \rangle$, while the off-diagonal elements $[\mathbf{\Gamma}^{-1}]_{ij}$ refer to the cross-correlations $\langle \Delta \mathbf{R}_i \cdot \Delta \mathbf{R}_j \rangle$. The proportionality constant between $[\mathbf{\Gamma}^{-1}]_{ij}$ and $\langle \Delta \mathbf{R}_i \cdot \Delta \mathbf{R}_j \rangle$ is simply $3k_BT/\gamma$, where k_B is the Boltzmann constant and T is the temperature.

Recent applications of the GNM approach to a series of proteins showed that the predicted $\langle \Delta \mathbf{R}_i^2 \rangle$ are in excellent agreement with the X-ray crystallographic temperature factors $B_i = 8\pi^2 \langle \Delta \mathbf{R}_i^2 \rangle / 3$ (Bahar et al., 1997). For illustrative purposes, the comparison of the B factors predicted by the GNM model (thick solid line) and experiment (thin solid line) is presented in Figure 2 for CI2, C2 protein isolated from *Paracoccus denitrificans*, and CheY. Furthermore, a strong correlation between hydrogen exchange free energy change measurements and GNM predictions was recently obtained for a series of proteins in their native states or under mild denaturing conditions (Bahar et al., 1998b). These comparisons support the use of GNM as a simple, yet physically reliable, means for characterizing the collective dynamics of proteins.

In the hydrogen exchange study, the free energy costs of exchange with the solvent for individual residues was shown to be inversely proportional to their MS fluctuations $\langle \Delta \mathbf{R}_i^2 \rangle$. The $\langle \Delta \mathbf{R}_i^2 \rangle$ values calculated therein result from the superposition of all N modes. Here, the dynamics is decomposed into N normal modes, and the shapes of the different modes are examined.

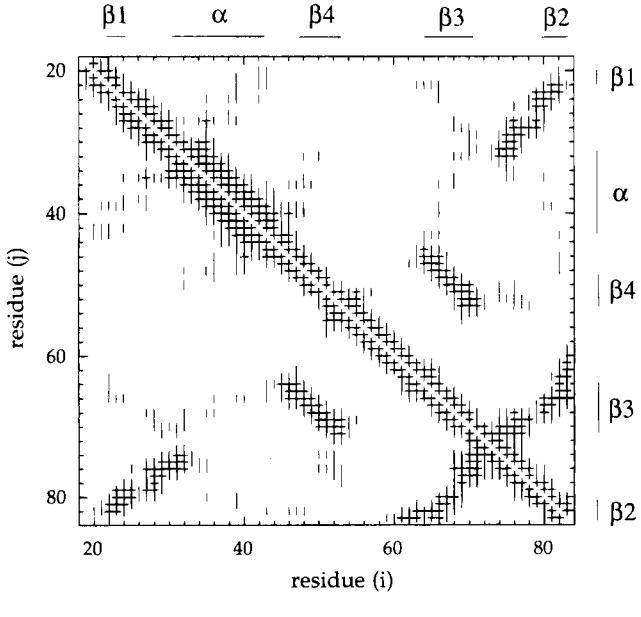

Fig. 1. Contact map for chymotrypsin inhibitor 2 (CI2). Secondary structure elements are shown along the axes. Horizontal and vertical bars on the map indicate the non-zero elements of $\mathbf{\Gamma}$ obtained from the crystal structure (McPhalen & James, 1987) (PDB code 2ci2) using the cutoff distances $r_c = 7$ and 10 Å, respectively. Residue indices along the two axes vary in the range $19 \leq i \leq 83 = N$.

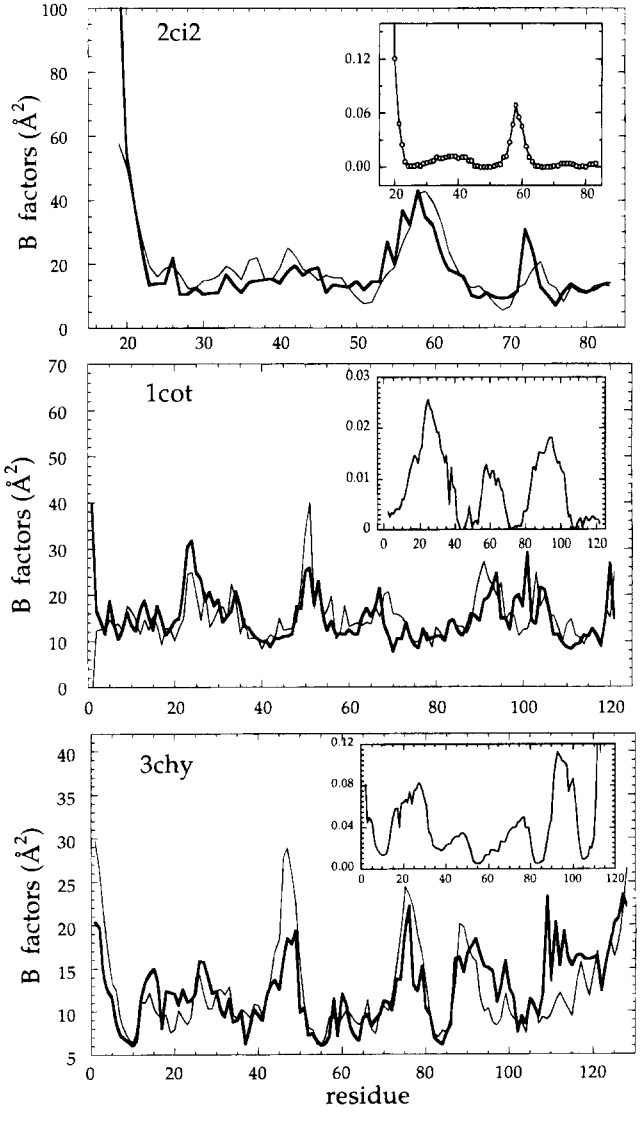

Fig. 2. Comparison of theoretical (thick curve) and experimental (thin curve) B factors for 2ci2, 1cot, and 3chy (see Table 1). The curves are normalized, i.e., the areas enclosed by both curves are equal. The inset displays the residue MS fluctuations driven by the slowest two modes. Smoother curves with peaks and minima corresponding to the most flexible and most restricted regions, respectively, in the global motions of the proteins are obtained by examining the slowest modes.

Dynamic fluctuation and correlation characteristics from GNM

The dynamic characteristics of a given structure are described in terms of (1) its natural frequencies and (2) the shapes of the corresponding modes of motion. In the GNM, the former is given by the eigenvalues λ_k, $2 \leq k \leq N$ of $\mathbf{\Gamma}$, excluding the zero eigenvalue λ_1, and the latter by the eigenvectors $\mathbf{u}_k$, $2 \leq k \leq N$. Thus, it suffices for elucidating the dynamics of a protein in the folded state, to decompose its $\mathbf{\Gamma}$ matrix into its eigenvalues and eigenvectors. The cross-correlation $\langle \Delta\mathbf{R}_i \cdot \Delta\mathbf{R}_j \rangle_k$ associated with the k^{th} mode of motion is (Bahar et al., 1997; Haliloglu et al., 1997)

$$\langle \Delta\mathbf{R}_i \cdot \Delta\mathbf{R}_j \rangle_k = (3k_BT/\gamma)[\lambda_k^{-1}\mathbf{u}_k\mathbf{u}_k^T]_{ij} = (3k_BT/\gamma)\lambda_k^{-1}[\mathbf{u}_k]_i[\mathbf{u}_k]_j. \quad (2)$$

Here the subscripts designate the elements of the matrices (or vectors) enclosed in brackets. In the following, we will be interested in the MS fluctuations of residues ($i = j$) in a given mode k. The problem thus reduces to the calculation of $[\mathbf{u}_k]_i$ as a function of i, for a given k, all other quantities in Equation 2 being invariant with respect to residue. The change in $[\mathbf{u}_k]_i$ with residue i is referred to as the k^{th} mode shape.

In general, the slowest modes give information on the global dynamics of the molecule (Bahar et al., 1998b). Domain movements or flexible loop motions, characterized by relatively longer correlation times, are identified by focusing on these modes (Holm & Sander, 1994), similarly to the common approach in normal mode analysis. Calculations for CI2, C2 protein from *P. denitrificans* and CheY yield the curves shown in the insets of Figure 2 for the MS fluctuations $\langle (\Delta\mathbf{R}_i)^2 \rangle_k$ of residues in the two slowest modes of motion. For example, a smooth curve with a single peak including residues 54–62 on the active (binding) loop (McPhalen & James, 1987) emerges in CI2, revealing the expected correspondence between global motion and function of the protein.

The fastest modes, on the other hand, reveal the residues subject to rapid, small amplitude fluctuations. Their high frequencies result from the steepness of the potential energy landscape surrounding their local minima. In the present study, we will concentrate on these modes. In contrast to slow modes, which occur cooperatively and cover segments of several contiguous residues along the backbone, fast modes affect individual residues, or residue pairs, which may be viewed as "hot spots," crucial for the stability of the structure, as explained below.

Chain connectivity vs. nonbonded contacts

In the extreme case of a highly extended chain conformation, no contacts apart from those between the nearest neighbors along the chain occur, and the Kirchhoff matrix $\mathbf{\Gamma}$ reduces to the classical tridiagonal Rouse matrix (Rouse, 1953), widely used for exploring the collective dynamics of polymers in the random coil state. The off-diagonal and the diagonal terms are -1 and 2, respectively, in this case. The only exception is the first and last diagonal elements, which are equal to one. This form of $\mathbf{\Gamma}$ represents the extreme case including solely the chain connectivity effect. The chain is conceived in this model as a linear sequence of springs with identical force constants γ, as illustrated in Figure 3A.

In globular structures, the one-dimensional geometric periodicity due to chain connectivity is broken by three-dimensional topological contacts. The matrix $\mathbf{\Gamma}$ displays a unique, irregular form for each protein, depending on the distribution of nonbonded contacts. The coupling of residue i to its nonbonded neighbors within a distance r_c may be represented by the spring constant κ_i, as illustrated in Figure 3B.

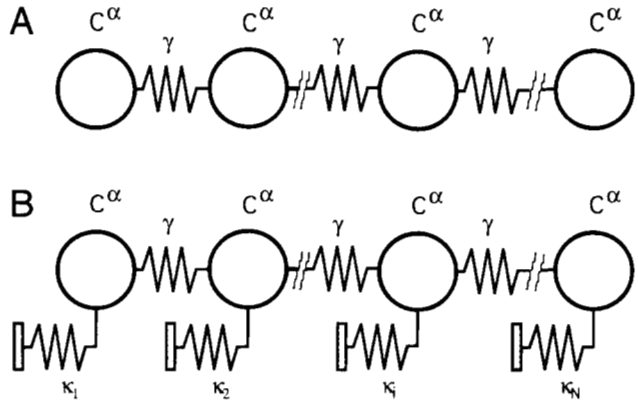

Fig. 3. A: Linear bead-and-spring model for a typical Rouse chain having no nonbonded contacts. Identical force constants γ are assigned to all bonds. This model leads to a tridiagonal Kirchhoff matrix. **B:** Model for a chain having nonbonded contacts. Each bead (or residue in proteins) is coupled to the bath formed by all nonbonded neighbors. κ_i is the equivalent coupling constant accounting for the nonbonded contacts of residue i. This model is obtainable by tridiagonalizing the corresponding Kirchhoff matrix.

An equivalent tridiagonal contact matrix may be created from the one that pertains to the native state of a protein. This is achieved by a Householder transformation, which reduces $\mathbf{\Gamma}$ to a tridiagonal form after a sequence of $N - 2$ orthogonal transformations. To quantify the extent of irregularity introduced by nonbonded contacts, we may examine for each residue the ratio of the diagonal to off-diagonal terms in the equivalent tridiagonal contact matrix, and compare it to the value -2 of the Rouse matrix. For the one-dimensional system shown in Figure 3B, this ratio is $-(2\gamma + \kappa_i)/\gamma = -2 - \kappa_i/\gamma$. Thus, the difference $-\kappa_i/\gamma$ for each residue with respect to the value -2 describes the disorder introduced by nonbonded contacts.

Figure 4 illustrates the highest frequency mode shapes evaluated for CI2. Curve A (thin line) displays the regular shape of the highest frequency mode obtained for the chain devoid of nonbonded interactions. This is obtained simply from the N^{th} eigenvector of the Rouse matrix of order N. Curve B (thick line), on the other hand, includes all nonbonded contacts between residue pairs separated by a distance $r_{ij} \leq r_c = 10$ Å. Here, the X-ray α-carbon coordinates of CI2 are used to construct $\mathbf{\Gamma}$, and the elements of the N^{th} eigenvector $[\mathbf{u}_N]_i$ of $\mathbf{\Gamma}$ are plotted. An extremely sharp peak at residue 68 is observed in curve B. This is a kinetically hot residue. This residue, together with Ile76, has been precisely pointed out to make tertiary contacts with the α-helical residue Ala35 buried in the core, and thus stabilize the folding nucleus of CI2 (Itzhaki et al., 1995; Fersht, 1997). Curve A, on the other hand, is devoid of such hot spots, due to the absence of tertiary contacts. It covers the whole spectrum obeying a short-wavelength periodicity.

The highest frequency mode shapes

The analysis performed above for the fastest mode may be repeated for a series of high frequency modes. This permits identi-

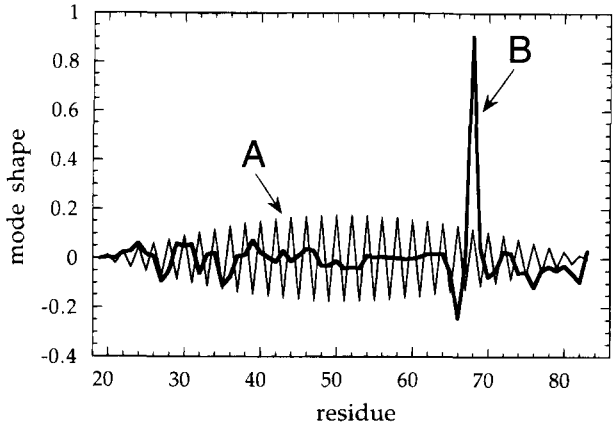

Fig. 4. The highest frequency mode shape for CI2, evaluated (**A**) in the absence of nonbonded interactions, obtained from the N^{th} eigenvector of the Rouse matrix of order N. **B:** In the presence of nonbonded contacts between residue pairs separated by a distance $r_{ij} \leq r_c = 10$ Å. A sharp peak at residue 68 is observed, indicating that this is a kinetically hot residue.

fication of the residues undergoing extremely short-wavelength motions. The results for the fastest seven modes $N - 6 \leq k \leq N$ (= 83) of CI2 are presented in Figure 5. Curves are individually scaled to the range $-1 \leq [\mathbf{u}_k]_i \leq 1$, and separated along the vertical axis for clarity.

The second fastest mode exhibits a sharp peak at Ile76, which was also pointed out to be participating in the folding nucleus of CI2. A further examination reveals that the key residues reported both theoretically and experimentally are all captured in the highest frequency modes. Mainly, we distinguish the α-helical residues Ala35 and Ile39, and residues Val66, Leu68, Phe69, Val70, and Ile76, which stabilize the former α-helix by tertiary contacts. Ala35, Leu68, Val70, and Ile76 have indeed been pointed out in several

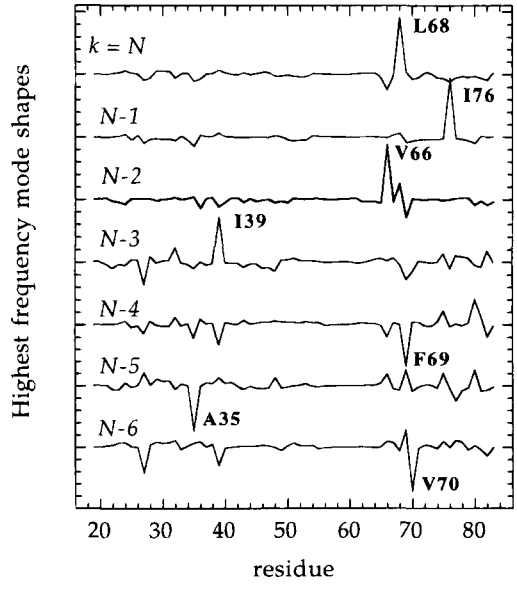

Fig. 5. The seven highest mode shapes evaluated for CI2. Significant peaks are indicated on the figure.

protein engineering studies of Fersht and collaborators to initiate folding and stabilize the folding nucleus (Itzhaki et al., 1995; Fersht, 1997). Wolynes and coworkers estimated the hot residues of CI2 from a correlation analysis of a theoretical transition state ensemble (Shoemaker et al., 1997). In addition to Ala35, Leu68, and Ile76, they calculated Ile39 to be highly sensitive to mutations, similarly to our results. Ile39 and Ala35 are on adjacent turns of the α-helix, which could explain the appearance of Ile39 among the set of hot residues. Likewise, the participation of Val66 and Phe69 among hot residues could result from the joint effect of chain connectivity (these being located on the same β-strand as Leu68 and Val70) and their tendency to be buried in the hydrophobic core.

In addition to these residues, there are weaker but noticeable peaks at residues Leu27 and Val32 participating in the type II reverse turn at the N-cap of the α-helix, and at Pro80, the first residue of the terminal β-strand, which raises the question of the possible role of kinetically hot residues for initiating or stopping secondary structural elements in native folds.

We note that the residues presently identified as the kinetically hot spots in CI2 are strongly correlated with those found by Shakhnovich et al. (1996) to be conserved among sequences designed to fold into the same conformation. The sequence variation entropy values were also calculated at these sites using the HSSP database sequence alignments (Sander & Schneider, 1991). Relatively low entropy values (≤0.30 after normalization to 1) are found for Ala35, Ile39, Val66, Val70, and Ile76. A correlation between residue conservation and kinetically hot spots is, therefore, clearly observed.

Results and discussion

Results and discussion for cytochrome and C2 proteins, and for CheY

An alternative way of examining the cumulative effect of the highest frequency modes is to combine the individual curves into a weighted average. From Equation 2, the MS fluctuations contributed by a given subset of modes $k_1 \leq k \leq k_2$ are

$$\langle (\Delta R_i)^2 \rangle_{k_1 - k_2} = (k_B T/\gamma) \sum_{k_1}^{k_2} \lambda_k^{-1} [\mathbf{u}_k]_i^2 \Big/ \sum_{k_1}^{k_2} \lambda_k^{-1}. \qquad (3)$$

In the following we will examine the MS fluctuations $\langle (\Delta R_i)^2 \rangle_{k_1 - k_2}$ induced by the modes $N - 4 \leq k \leq N$ in the proteins listed in Table 1. Representative results obtained using $r_c = 7.0$ Å are displayed in Figure 6. Figure 6A displays the results for CI2, Figure 6B for horse cytochrome *c*, Figure 6C for protein C2 isolated from *P. denitrificans*, and Figure 6D for CheY. The fluctuation distributions are normalized, i.e., the MS values are divided by $3k_BT/\gamma$ so that the area enclosed by each curve is equal to unity. Peaks refer to kinetically hot residues. Usually one sharp peak is associated with each mode, as may be seen in Figure 5 for CI2, although two weaker peaks also appear in a few cases. This leads to about six peaks per protein in the cumulative distributions obtained for the five fastest modes, as listed in Table 2.

Ribbon diagrams of some representative proteins are shown in Figure 7. Therein, the residues identified as the kinetically hot spots, and hence implicated in possible nucleation-condensation mechanisms, are shown in red. Most of these residues make pair-

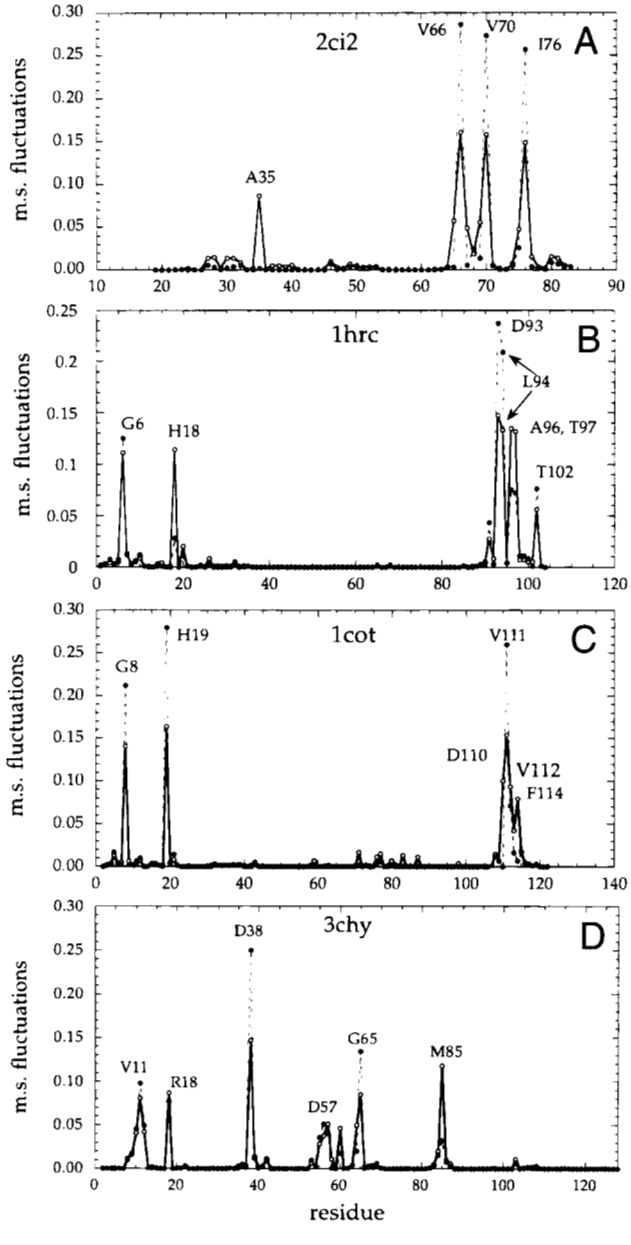

Fig. 6. Mean-square fluctuations of residues driven by the subset of the highest five frequency modes, displayed for (**A**) 2ci2, (**B**) 1hrc, (**C**) 1cot, and (**D**) 3chy (see Table 1). Results are obtained using Equation 3 with r_c = 7 Å. The distributions are normalized. Peaks indicate the hot residues. The results for the highest three modes ($N - 2 \leq k \leq N$) are also displayed by the thin dashed curves.

wise contacts or form clusters ($r_{ij} \leq r_c$ = 7 Å) in the folded state (Table 2). Contacts between hot residues are indicated by the yellow dashed lines in the figure.

The kinetically hot residues coincide with the tightly packed regions of the folded structures. Their coordination numbers are generally above 10, on the basis of all α-carbons within a spherical shell of 7 Å in the neighborhood of a central α-carbon. However, consideration of coordination numbers alone does not discriminate between residues exhibiting the same local packing density but different types of coordination order. Examples were observed in which residues having the same local packing density exhibited distinct fluctuation behavior. In the C2 protein (1cot) for example, residues 20 and 71 are not observed among the hot residues, although their coordination number (12) is equal to that of hot residues 110, 112–114.

Cytochrome c and related C2 proteins

Calculations performed for cytochrome *c* and related C2 proteins listed in Table 1 show that the two terminal helices, or more precisely a few specific residues in these helices, are distinguished by sharp peaks in the high frequency mode distributions (Fig. 6). The normalized MS fluctuations for horse cytochrome *c* (1hrc) residues are displayed in Figure 6B, as representative of other cytochrome *c*'s (e.g., tuna, bonito, yeast) that are closely superimposable both spatially and sequentially. The curve for the C2 protein (1cot) is displayed in Figure 6C. The results for the other proteins in this group (1ccr, 1cry, 5cyt, and 3c2c) are summarized in Table 2.

In all cases, the set of hot residues comprise a glycine (G6 or G8) in the N-terminal α-helix, four or five residues in the C-terminal helix, together with a histidine (or a tryptophan in 1cry, and a methionine in 3c2c), which ligate the iron atom at the center of the heme group in the central portion of the molecule. The C-terminal helix is the most stable region in native cytochrome *c* (Bai et al., 1995) possessing helical structure even in isolated form, which is consistent with the appearance of several residues belonging to this helix in Table 2. The key residues of this helix generally lie between an aspartic acid (or asparagine in 1cxa and 3c2c) at one end, and an aromatic residue, Phe or Tyr, at the other. These might form the embryonic secondary structure, or nucleus, to be stabilized by tertiary contacts. In fact, close contacts with the hot residues G6 or G10 occur in the folded state, forming the clusters listed in the last column of Table 2. The histidines do not participate in these clusters. Although the residue indices differ therein, sequence alignments using matrices of contacts demonstrate (Ptitsyn, 1998) that the residues participating in these clusters are equivalent, i.e., have the same geometry of contacts in all five cases.

The packing of residues in the C- and N-terminal helices is known to play a critical role in the kinetics of folding (Elöve et al., 1992; Colón et al., 1996). These helices acquire about 60% protection within the 20 ms burst phase of refolding (Roder et al., 1988), and also control the global unfolding of the molecule (Bai et al., 1995; Englander et al., 1997). In particular, the L94A mutation is observed to block all folding steps after the initial collapse (Colón & Roder, 1996), in conformity with the present identification of L94 as a kinetically important residue. The acid-denatured form (A-form) of cytochrome is stabilized by the interactions between the conserved residues at the interface of these helices (e.g., Gly6–Leu94) (Marmorino & Pielak, 1995). Our recent GNM calculations of hydrogen exchange free energy changes for cytochrome *c* also revealed the dominant role of the presently identified hot residues (Bahar et al., 1998b).

Apart from the few residues at the terminal helices, our calculations indicate the important role of a histidine, or tryptophan, buried near the heme-binding site. The His residue at position 19 (or 18 in 1hrc) has a very low sequence variation entropy (≤0.06 after normalization to 1) as determined from HSSP database sequence alignments (Sander & Schneider, 1991), which indicates strong conservation at this position. We note that Raman scattering measurements coupled with submillisecond mixing techniques also

Table 2. *Kinetically hot residues and their clusters/contacts in the folded state*

PDB code	Kinetically hot residues[a]	Clusters/contacts[b]
2ci2	A35*, V66, L68*, V70*, I76*	{68, 70, 76}, (66,68)
1hrc	G6*, H18*, D93, L94*, A96, Y97*	{6, 93, 94, 96, 97}
1ccr	G14*, H26*, A100, D101, L102*, S104, Y105*	{14,101,102,104,105}, {100,101,102,104,105}
1cot	G8*, H19*, D110, V111*, V112, F114*	{8, 110, 111, 112, 114}
1cxa	G8*, H19*, N112, I113*, A115, Y116*	{8, 112, 113, 115, 116}
1cry	G6*, W58, D92, L93*, A95, F100, N101	{6, 92, 93}, {100,101}
5cyt	G6*, H18, D93, L94*, A96, Y97*	{6,93,94,96,97}
3c2c	G7*, H18, M55, N103,V104*, A106, T107*	{7,103,104,106,107}
3chy	V11*, R18, D38, D57*, D64, G65*, M85*	(11,18), (11,38), (11,57), (57,65), (57,85)

[a]Residues whose normalized MS fluctuations in the high frequency modes are above $6N^{-1}$. See Figure 6. Highly conserved residues are indicated by an asterisk.

[b]Clusters are shown in braces. Each pair of residues in a cluster is separated by ≤7 Å. Contacts, shown in parentheses, refer to pairs within 7 Å. Distances refer to α-carbon separations.

showed the important role of histidine heme-ligand interactions, and the possible trapping in a misligated form determining folding kinetics (Takahashi et al., 1997; Yeh et al., 1997), in parallel with earlier observations (Elöve et al., 1992).

As a final remark, we note that the kinetically hot residues listed in the last column of Table 2 exhibit a close correlation with the most conserved residues recently identified for the same proteins (Ptitsyn, 1998). Residues G6, F10, L94, and Y97 in 1hrc, G14,

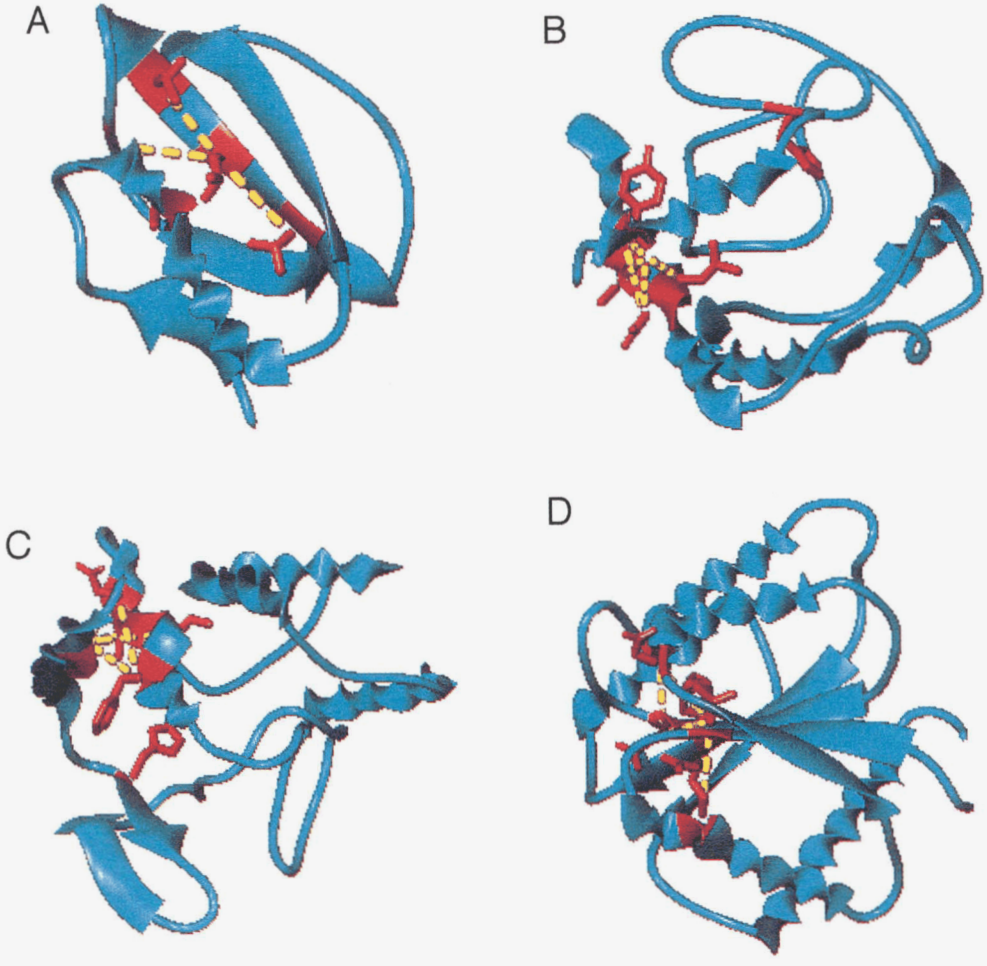

Fig. 7. Ribbon diagrams of 2ci2, 1hrc, 1cot, and 3chy. The residues presently identified as the kinetically hot residues are shown in red. Contacts between hot residues are indicated by yellow dashed lines.

F18, L102, and Y105 in 1ccr, G8, F12, V111, F114 in 1cot, G6, F10, L93, Y96 in 1cry, and G8, F12, I113, and Y116 in 1cxa were pointed out to be the most conserved four residues in the group examined (Ptitsyn, 1998). And among these four residues, generally three are identified by GNM as kinetically hot. These are indicated by the asterisks in the second column of Table 2. The phenylalanine residue in the N-terminal helix does not appear in the present GNM calculations to be active in the fastest modes. A plausible explanation is that the aotual packing density near this and other large residues is somewhat underestimated by the definition of contacts taken here. GNM calculations repeated by considering atomic contacts indeed yield a sharp peak at the position of the mentioned Phe residues. For example, in 1cot, Phe12 emerged as the highest peak succeeding D110 when the force constant γ associated with inter-residue interactions was rescaled with the number of atom–atom contacts within 6.0 Å. This observation suggests a possible direction for improving the GNM model in future studies.

Results for CheY

CheY is an α/β bacterial signal transduction protein of 129 amino acids from *E. coli* (Stock et al., 1990). It contains two subdomains: the first includes the first two β-strands (residues 7–11 and 32–36) and two α-helices (15–26 and 39–46), and the second the remaining three β-strands (53–57, 82–87, and 106–108) and three α-helices (65–73, 92–99, and 113–125). It is reported that the structure of the first subdomain in the transition state resembles that observed for CI2 (López-Hernández & Serrano, 1996) and the second subdomain is unstable until the first has folded (Muñoz et al., 1994; López-Hernández & Serrano, 1996).

The folding pathway of CheY exhibits a kinetic intermediate as does cytochrome *c*. However, the results of the present method as presented in Figures 6D and 7D indicate that the structure of the core formed by the hot residues is different from that of cytochrome *c*. Essentially, the hot residues are distributed over a broader distance range, compared to those in cytochrome *c* that are precisely located at the terminal helices. To clarify the distinction, we show in Figure 8 a ribbon diagram of CheY, in which the kinetically hot residues are explicitly labeled, and the two subdomains, the first shown in blue and the second in gray, are distinguished. The kinetically hot residues consists of two subgroups, each composed of three residues. The former three, V11, R18, and D38, located in the first subdomain (lower part), are shown in red, and those in the second subdomain, D57, G65, and M85, are shown in green. The nonlocal interaction between V11 and D57 establishes the communication between the hot residues of the two subdomains.

López-Hernández and Serrano (1996) found that the packing of the first α-helix against the first two β-strands forms the nucleus around which CheY folds. The nucleus mentioned in that study may be associated with the first group of hot residues presently found. However, a second group of residues, located in the second subdomain, is identified in our approach. It is interesting to observe that the key residue D57, which is presently shown to be active in the communication of the two subgroups of hot residues in the different domains, is found by Stock et al. (1990) to be highly conserved among the family of bacterial signal transduction proteins including CheY. Two other highly conserved residues are shown therein to be D13 and K109; also, stretches of residues forming a conserved hydrophobic core are reported. The latter includes the kinetically hot residues V11 and M85 presently identified. Besides, we note that G65 is also conserved among all of the 20 reported homologous regions of response regulators aligned against CheY, except one in which it is replaced by Ala, and that residue 38 exhibits a strong preference to be aspartic acid or asparagine. We also note that the sequence variation entropy values for D57 and G65 calculated from the HSSP database (Sander & Schneider, 1991) are identically zero, the residue identity at these two positions being completely conserved in all aligned sequences.

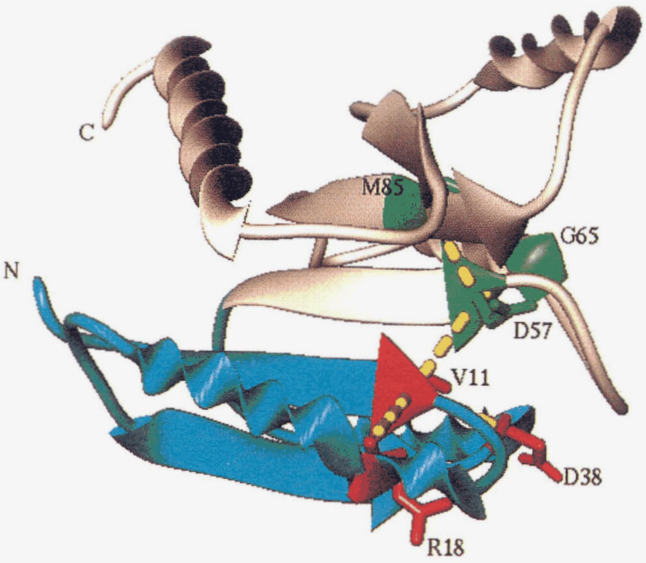

Fig. 8. Ribbon diagram of CheY (PDB entry 3chy). The residues found as kinetically hot are shown in red and green, located in the first (blue) and the second (gray) subdomains, respectively. Tertiary contacts between the hot residues are marked by yellow dashed lines. The bridge between the nuclei is established by the V11-D57 nonlocal interaction.

Conclusion

In the present study, a systematic method for identifying the kinetically hot residues in folded proteins, is presented, based on the GNM of proteins. These are generally tightly packed residues. Thus, the coordination number of individual residues is an important property dominating the fluctuation behavior. In addition to their relatively high local packing density, residues presently identified as hot spots experience an extremely strong coupling to all other residues within the particular network topology of native nonbonded contacts. They are distinguished after decomposition of the protein dynamics into a set of collective modes, and examination of the residue fluctuations driven by the highest frequency/smallest amplitude modes.

The occurrence of high frequency modes is associated with the steepness of the energy landscape in the neighborhood of the local minima corresponding to the equilibrium (native) positions of residues. Any departure from these mean positions is strongly opposed due to the steepness of the surrounding energy walls. Such centers cannot efficiently exchange energy with their surroundings, and thus preserve their state despite changes in other parts of the structure, which suggests their possible involvement at the nucleation-condensation stage of folding. Our recent study of hydrogen exchange behavior also showed that residues subject to

small amplitude/high frequency fluctuations cannot efficiently exchange with the solvent (Bahar et al., 1998b).

The residues listed in Table 2 and displayed in Figure 7 are identified from application of the GNM method to CI2, cytochrome *c*, and related C2 proteins. Most of these residues were pointed out in previous theoretical and experimental studies to be crucial for the formation and/or stability of the tertiary fold. They either participate in the formation and stabilization of a folding nucleus, as in CI2 obeying a two-state folding kinetics, or exhibit native-like contacts in the intermediate or molten globule states formed on the folding pathway. Examples of the latter case are cytochrome *c* and CheY. Thus, irrespective of the folding mechanism, it is possible to describe a nucleus or core that consists of relatively small numbers of residues forming native-like contacts. As recently pointed out by Ptitsyn (1996), the tightly packed regions in intermediates may include the folding nuclei, or coincide with them. Furthermore, even proteins unfolding via a noncooperative mechanism may exhibit a core, or a nucleus, preserving its native structure, as observed in recent NMR experiments of α-lactalbumin unfolding by Schulman et al. (1997). Therein a core region that remains collapsed under extreme denaturing conditions is detected, which supports a model in which the core provides a template for the correct assembly of the remainder of the structure.

To conclude, the present method identifies the residues, pairs or clusters, which exhibit highly stabilized, key interactions, in tertiary folds. These residues correlate with those previously pointed out to play an important role in the initiation of folding, suggesting that the localization of energy in the neighborhood of these residues may be traced back to earlier folding stages, i.e., to the passage over a transition state or intermediate states in which the same tertiary contacts are formed. The further correlation between these residues and those found to be conserved in different members of a given family or in different engineered proteins, as demonstrated above for CI2, CheY, cytochrome *c*, and related C2 proteins is consistent with the need to preserve key interactions underlying stability during evolution or protein engineering.

Acknowledgments

Partial support from Bogazici University Research Funds A970401 and NATO Collaborative Research Grant Project #CRG951240 is gratefully acknowledged.

References

Abkevich VI, Gutin AM, Shakhnovich EI. 1994. Specific nucleus as the transition state for protein folding: Evidence from the lattice model. *Biochemistry 33*:10026–10036.

Anderson PW. 1958. The absence of diffusion in certain random lattices. *Phys Rev 109*:1492–1505.

Anderson PW. 1978. Local moments and localized states (Nobel lectures in physics for 1977). *Rev Mod Phys 50*:191–201.

Axelrod HL, Feher G, Rees DC. 1994. Crystallization and X-ray structure determination of cytochrome c2 from *Rhodobacter sphaeroides* in three crystal forms. *Acta Crystallog Sect D Biol Crystallog 50*:596–602.

Bahar I, Atilgan AR, Demirel MC, Erman B. 1998a. Vibrational dynamics of folded proteins: Significance of slow and fast modes in relation to function and stability. *Phys Rev Lett 80*:2733–2736.

Bahar I, Atilgan AR, Erman B. 1997. Direct evaluation of thermal fluctuations in proteins using a single parameter harmonic potential. *Fold Design 2*:173–181.

Bahar I, Jernigan RL. 1997. Inter-residue potentials in globular proteins and the dominance of highly specific hydrophilic interactions at close separation. *J Mol Biol 266*:195–214.

Bahar I, Wallquist A, Covell D, Jernigan RL. 1998b. Correlation between native state hydrogen exchange and cooperative residue fluctuations from a simple model. *Biochemistry 37*:1067–1075.

Bai Y, Sosnick T, Mayne L, Englander SW. 1995. Protein folding intermediates studied by native-state hydrogen exchange. *Science 26*:192–197.

Benning MM, Meyer TE, Holden HM. 1994. X-ray structure of the cytochrome c2 isolated from *Paracoccus denitrificans* refined to 1.7 Ångstroms resolution. *Arch Biochem Biophys 310*:460–466.

Bushnell GW, Louie GV, Brayer GD. 1990. High-resolution three-dimensional structure of horse heart cytochrome *c*. *J Mol Biol 214*:585–595.

Colón W, Elöve GA, Wakem LP, Sherman F, Roder H. 1996. Side chain packing of the N- and C-terminal helices plays a critical role in the kinetics of cytochrome *c* folding. *Biochemistry 35*:5538–5549.

Colón W, Roder H. 1996. Kinetic intermediates in the formation of the cytochrome *c* molten globule. *Nature Struct Biol 3*:1019–1025.

Daggett V, Li AJ, Itzhaki LS, Otzen DE, Fersht AR. 1996. Structure of the transition state for folding of a protein derived from experiment and simulation. *J Mol Biol 257*:430–440.

Dean P, Bacon MD. 1963. The nature of vibrational modes in disordered systems. *Proc Phys Soc 81*:642–647.

Dill KA, Bromberg S, Yue K, Fiebig KM, Yee DP, Thomas PD, Chan, HS. 1995. Principles of protein folding. A perspective from simple exact models. *Protein Sci 4*:561–602.

Elöve GA, Chaffotte AF, Roder H, Goldberg ME. 1992. Early steps in cytochrome *c* folding probed by time-resolved circular dichroism and fluorescence spectroscopy. *Biochemistry 31*:6876–6883.

Englander SW, Mayne L, Bai Y, Sosnick TR. 1997. Hydrogen exchange: The modern legacy of Linderstrøm-Lang. *Protein Sci 6*:1101–1109.

Fersht AR. 1997. Nucleation mechanisms in protein folding. *Curr Opin Struct Biol 7*:3–9.

Fersht AR, Itzhaki LS, ElMasry NF, Matthews JM. 1994. Single versus parallel pathways of protein folding and fractional formation of structure in the transition state. *Proc Natl Acad Sci USA 91*:10426–10429.

Haliloglu T, Bahar I, Erman B. 1997. Gaussian dynamics of folded proteins. *Phys Rev Lett 79*:3090–3093.

Holm L, Sander C. 1994. Parser for protein folding units. *Proteins 19*:256–268.

Itzhaki LS, Otzen DE, Fersht AR. 1995. The structure of the transition state for folding of chymotrypsin inhibitor 2 analyzed by protein engineering methods: Evidence for a nucleation condensation mechanism for protein folding. *J Mol Biol 254*:260–288.

Jackson SE, ElMasry N, Fersht AR. 1993. Structure of the hydrophobic core in the transition state for folding of chymotrypsin inhibitor 2: A critical test of the protein engineering method of analysis. *Biochemistry 32*:11270–11278.

Jeng MF, Englander SW. 1991. Stable submolecular folding units in noncompact form of cytochrome *c*. *J Mol Biol 221*:1045–1061.

Karplus M, Sali A, Shakhnovich E. 1995. Kinetics of protein folding. *Nature 373*:664–665.

Kataoka M, Hagihara Y, Mihara K, Goto Y. 1993. Molten globule of cytochrome *c* studied by small angle X-ray scattering. *J Mol Biol 229*:591–596.

Kim PS, Baldwin RL. 1990. Intermediates in the folding reactions of small proteins. *Annu Rev Biochem 59*:631–660.

Kuroda Y, Endo A, Nagayama K, Wada A. 1995. Stability of α-helices in a molten globule state of cytochrome *c* by hydrogen/deuterium exchange and two-dimensional NMR spectroscopy. *J Mol Biol 247*:682–688.

Li AJ, Daggett V. 1996. Identification and characterization of the unfolding transition state of chymotrypsin inhibitor 2 by molecular dynamics simulations. *J Mol Biol 257*:412–429.

López-Hernández I, Serrano L. 1996. Structure of the transition state for the folding of the 129-amino acid protein CheY resembles that of the smaller protein CI2. *Fold Design 2*:43–55.

Marmorino JL, Pielak GJ. 1995. A native tertiary interaction stabilizes the A state of cytochrome *c*. *Biochemistry 34*:3140–3143.

McPhalen CA, James MNG. 1987. Crystal and molecular structure of the serine proteinase inhibitor CI-2 from barley seeds. *Biochemistry 26*:261–269.

Miki K, Sogabe S. 1995. Refined crystal structure of ferrocytochrome C2 from *Rhodopseudomonas viridis* at 1.6 Å resolution. *J Mol Biol 252*:235–247.

Miyazawa S, Jernigan RL. 1996. Residue-residue potentials with a favorable contact pair term and an unfavorable high packing density term, for simulation and threading. *J Mol Biol 256*:623–644.

Muñoz V, Lopez E, Serrano L. 1994. Kinetic characterization of the chemotactic protein from *E. coli* CheY. Kinetic analysis of the inverse hydrophobic effect. *Biochemistry 33*:5858–5866.

Neira JL, Itzhaki LS, Otzen DE, Davis B, Fersht AR. 1997. Hydrogen exchange in chymotrypsin inhibitor 2 probed by mutagenesis. *J Mol Biol 270*:99–110.

Ochi H, Hata Y, Tanaka N, Kakudo M, Sakurai T, Aihara S, Morita Y. 1983. Structure of rice ferricytochrome c at 2.0 Ångstrom resolution. *J Mol Biol 166*:407–418.

Otzen DE, Itzhaki LS, ElMasry NF, Jackson S, Fersht, AR. 1994. Structure of

the transition state for the folding/unfolding of the barley chymotrypsin inhibitor 2 and its implications for mechanisms of protein folding. *Proc Natl Acad Sci USA 91*:10422–10425.
Press WH, Teukolsky SA, Vetterling WT, Flannery BP. 1992. *Numerical recipes in Fortran: The art of scientific computing*, 2nd ed. Cambridge, UK: Cambridge University Press. 59 pp.
Ptitsyn O. 1998. Protein folds, and protein evolution: Common folding nucleus in different subfamilies of C-type cytochromes? *J Mol Biol 278*:655–666.
Ptitsyn OB. 1995. Molten globule and protein folding. *Adv Protein Chem 47*:83–229.
Ptitsyn OB. 1996. How molten is the molten globule? *Nature Struct Biol 3*:488–490.
Ptitsyn OB, Rashin AA. 1975. A model of myoglobin self-organization. *Biophys Chem 3*:1–20.
Roder H, Elöve GA, Englander SW. 1988. Structural characterization of folding intermediates in cytochrome *c* by H-exchange labeling and proton NMR. *Nature 335*:700–704.
Rouse PE. 1953. A theory of the linear viscoelastic properties of dilute solutions of coiling polymers. *J Chem Phys 21*:1272–1280.
Salemme FR, Freer ST, Xuong NH, Alden RA, Kraut J. 1973. The structure of oxidized cytochrome C2 of *Rhodospirillum rubrum*. *J Biol Chem 248*:3910–3921.
Sander C, Schneider R. 1991. Database of homology derived protein structures and the structural meaning of sequence alignment. *Proteins 9*:56–68.
Sayar M, Demirel MC, Atilgan AR. 1997. Dynamics of disordered structures: Effect of nonlinearity on the localization. *J Sound Vib 205*:372–379.
Schmid FX. 1992. Kinetics of unfolding and refolding of single-domain proteins. In: Creighton TE, ed. *Protein folding*. New York: W.H. Freeman and Company. pp 197–241.
Schulman BA, Kim PS, Dobson CM, Redfield C. 1997. A residue-specific NMR view of the non-cooperative unfolding of a molten globule. *Nature Struct Biol 4*:630–634.
Shakhnovich E, Abkevich V, Ptitsyn O. 1996. Conserved residues and the mechanism of protein folding. *Nature 379*:96–98.
Shoemaker BJ, Wang J, Wolynes PG. 1997. Structural correlations in protein folding funnels. *Proc Natl Acad Sci USA 94*:777–782.
Sosnick TR, Mayne L, Englander SW. 1996. Molecular collapse: The rate-limiting step in two-state cytochrome *c* folding. *Proteins 24*:413–426.
Stock JB, Stock AM, Mottonen JM. 1990. Signal transduction in bacteria. *Nature 344*:395–400.
Takahashi S, Yeh S-Y, Das TK, Chan C-K, Gottfried DS, Rousseau DL. 1997. Folding of cytochrome *c* initiated by submillisecond mixing. *Nature Struct Biol 4*:44–50
Takano T. 1984. *Refinement of myoglobin and cytochrome c*. Oxford, UK: Oxford University Press.
Tirion MM. 1996. Large amplitude elastic motions in proteins from a single-parameter, atomic analysis. *Phys Rev Lett 77*:1905–1908.
Volz K, Matsumura P. 1991. Crystal structure of *E. coli* Che-Y refined at 1.7 Ångstrom resolution. *J Biol Chem 266*:15511–15519.
Yeh S-R, Takahashi S, Baochen F, Rousseau DL. 1997. Ligand exchange during cytochrome *c* folding. *Nature Struct Biol 4*:51–56.
Zwanzig R. 1997. Two-state models of protein folding kinetics. *Proc Natl Acad Sci USA 94*:148–150.

Appendix

The GNM calculations are illustrated here for a simple model of eight residues. We consider the following model protein on a square lattce

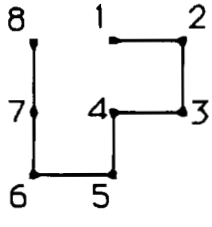

A quadratic form of energy is assumed for the fluctuation of all residues, in which the interactions between all "contacting" sites are represented with the same single parameter. Contacting residues are those located on adjacent sites, bonded, or nonbonded. The corresponding Kirchhoff matrix $\mathbf{\Gamma}$, defined by Equation 1, is

$$\mathbf{\Gamma} = \begin{bmatrix} 3 & -1 & 0 & -1 & 0 & 0 & 0 & -1 \\ -1 & 2 & -1 & 0 & 0 & 0 & 0 & 0 \\ 0 & -1 & 2 & -1 & 0 & 0 & 0 & 0 \\ -1 & 0 & -1 & 4 & -1 & 0 & -1 & 0 \\ 0 & 0 & 0 & -1 & 2 & -1 & 0 & 0 \\ 0 & 0 & 0 & 0 & -1 & 2 & -1 & 0 \\ 0 & 0 & 0 & -1 & 0 & -1 & 3 & -1 \\ -1 & 0 & 0 & 0 & 0 & 0 & -1 & 2 \end{bmatrix} \tag{4}$$

The eigenvalues (λ_k) and eigenvectors ($\mathbf{u}_k$) of $\mathbf{\Gamma}$, $1 \le k \le 8$, are computed using a standard eigenvalue decomposition subroutine (Press et al., 1992). The eigenvalues are found to be 0, 0.75, 1.28, 2.45, 2.52, 3.44, 3.80, 5.76, in ascending order. The latter refers to the highest frequency mode, and $\lambda_2 = 0.75$ is associated with the slowest mode. The zero eigenvalue is due to the translational invariance of the system. In other words, the elements of $\mathbf{\Gamma}$ depend on the distances between the residues, only; they are not altered during rigid body motion. In the evaluation of the B factors, the inverse of $\mathbf{\Gamma}$ is obtained after eliminating the zero eigenvalue, i.e., $\langle \Delta\mathbf{R}_i \cdot \Delta\mathbf{R}_j \rangle = \mathbf{\Sigma}_k \langle \Delta\mathbf{R}_i \cdot \Delta\mathbf{R}_j \rangle_k$, where the summation is performed over all nonzero eigenvalues ($2 \le k \le 8$), and the contribution of the k^{th} mode is given by Equation 2.

The eigenvectors corresponding to this simple model are plotted in Figure 9. The ordinate values are not explicitly shown, as the shapes, rather than the absolute values, are of interest. The absolute values may be readily found using $\Sigma_i [\mathbf{u}_k]_i^2 = 1$ for each eigenvector $\mathbf{u}_k$. Here $[\mathbf{u}_k]_i$ is the i^{th} element (associated with the i^{th} residue) of $\mathbf{u}_k$. The eigenvector associated

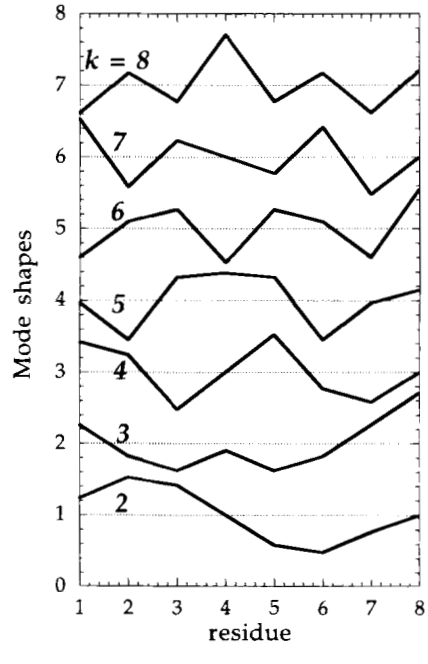

Fig. 9. Mode shapes for the simple on-lattice structure presented in the Appendix. The curves display the eigenvectors $\mathbf{u}_k$, $2 \le k \le 8$, as a function of residue index. Each element $[\mathbf{u}_k]_i$ of a given eigenvector $\mathbf{u}_k$ corresponds to a given residue (i) along the abscissa.

with the zero eigenvalue (λ_1), which is a straight line, is not shown. The eigenvector for the second smallest eigenvalue ($k = 2$) reflects the cooperative motion of the molecule. The fastest mode shape ($k = 8$), on the other hand, exhibits a pronounced peak at the fourth residue, the kinetically hot residue in the present simple model. This is the most tightly packed residue in the present simple model. For molecules with a larger number of residues, the mode shapes associated with the higher frequencies display sharper peaks at hot loci, as shown for CI2, for instance, in Figure 4, and are affected by the specific tertiary contacts, in addition to packing density. The general shapes closely resemble the modes of a vibrating string, in having approximately $k - 1$ axis crossings for mode k.

The FORTRAN code for calculating the B factors of PDB structures using GNM, and for evaluating the shapes of all modes is available on the internet (http://klee.bme.boun.edu.tr/code.f).